International Journal of Applied Mathematics & Statistics,
Int. J. Appl. Math. Stat.; Vol. 26; Issue No. 2; Year 2012,
ISSN 0973-1377 (Print), ISSN 0973-7545 (Online)

Chaos and complexity in the classical-quantum transition

A. M. Kowalski[1,4], **M. T. Martín**[1,5], **A. Plastino**[1,5] **and O. A. Rosso**[2,3,5]

[1]Instituto de Física, Facultad de Ciencias Exactas
Universidad Nacional de La Plata
C.C. 67, 1900 La Plata, Argentina
kowalski@fisica.unlp.edu.ar; mtmartin@fisica.unlp.edu.ar;
plastino@fisica.unlp.edu.ar

[2]Departamento de Física, Instituto de Ciências Exatas
Universidade Federal de Minas Gerais
Av. Antônio Carlos, 6627 - Campus Pampulha
CEP 31.270-901, Belo Horizonte, MG, Brazil
oarosso@fibertel.com.ar, oarosso@gmail.com

[3]Chaos & Biology Group, Instituto de Cálculo
Facultad de Ciencias Exactas y Naturales, Universidad de Buenos Aires
Pabellón II, Ciudad Universitaria
1428 Ciudad Autonoma de Buenos Aires, Argentina

[4]Comisión de Investigaciones Científicas (CICPBA), Argentina

[5]Consejo Nacional de Investigaciones Científicas y Técnicas (CONICET), Argentina

ABSTRACT

By recourse to the concept of Statistical Complexity we study here the classical-quantum transition in a special system that represents the matter-field interaction. Our work considers two distinct disequilibrium forms based on Euclidean norm and Jensen-Shannon divergence, on the one hand, and analyzes things, on the other one, by using two different numerical approaches for probability distribution, namely, relative wavelet energy and permutation patterns.

Keywords: Semiclassical theories, quantum chaos, statistical complexity.

PACS: 03.65.Sq (Semiclassical theories and applications), 05.45.Mt (Quantum chaos; semiclassical methods) 05.45.Tp (Time series analysis)

1 Introduction

Since the introduction of the decoherence concept in the early 1980s, by, among others, Zeh, Zurek, and Habib (Zeh, 1999; Zurek, 1981; Zurek, 2003; Zurek, Habib and Paz, 1993; Habib, Shizume and Zurek, 1998), the emergence of the classical world from Quantum Mechanics has

been a subject of much interest. Among the associated issues one can mention the emergence of classical dynamics (specially classical chaos) in quantum systems through continuous measurement, observed by Habib, Bhattacharya, Ghose, and Jacobs, among others (Ghose, Alsing, Deutsch, Bhattacharya, Habib and Jacobs, 2003; Ghose, Alsing, Deutsch, Bhattacharya and Habib, 2004) and the "decoherent histories approach" by Gisin, Brun, Halliwell, and Percival (Diósi, Gisin, Halliwell and Percival, 1995; Brun and Halliwell, 1996; Brun, 2000; Halliwell and Yearsley, 2009). Additionally, authors like Everitt explore the quantum-classical crossover in the behavior of a quantum field mode (Everitt, Munro and Spiller, 2009) and the chaotic-like and non-chaotic-like behavior in nonlinear quantum systems (Everitt, 2007), topics of certain interest. One should also consult papers by Ralph et al. (Clark, Diggins, Ralph, Everitt, Prance, H., Whiteman, Widom and Srivastava, 1998), Greenbaum et al. (Greenbaum, Habib, Shizume and Sundaram, 2005) and Lifshitz et al. (Katz, Retzker, Straub and Lifshitz, 2007).

It is clear that quite a bit of quantum insight is to be gained from semiclassical perspectives. Several methodologies are available (WKB, Born-Oppenheimer approach, etc.). The model of Refs. (Bonilla and Guinea, 1992; Cooper, Dawson, Habib and Ryne, 1998; Kowalski, Plastino and Proto, 2002) considers two interacting systems: one of them classical, the other quantal. This makes sense whenever the quantum effects of one of the two systems are negligible in comparison to those of the other one. Examples can be readily found. We can just mention Bloch equations (Bloch, 1946), two-level systems interacting with an electromagnetic field within a cavity (Milonni, Shih and Ackerhalt, 1987; Meystre and Sargent III, 1991; Kociuba and Heckenberg, 2002), collective nuclear motion (Ring and Schuck, 1980), etc.

Quantifiers based on information theory, like entropic forms and statistical complexities (see as examples Refs. (Shannon, 1948; Shiner, Davison and Landsberg, 1999; López-Ruiz, Mancini and Calbet, 1995; Lamberti, Martín, Plastino and Rosso, 2004)) have proved to be very useful in the characterization of the dynamics associated to time series, in the wake of the pioneering work of Kolmogorov and Sinai, who converted Shannon's information theory into a powerful tool for the study of dynamical systems (Kolmogorov, 1958; Sinai, 1959). In turn, information theory measures and probability spaces Ω are inextricably linked quantifiers. In evaluating them, the determination of the probability distribution P associated to the dynamical system or time series under study is the basic ingredient. Many procedures have been proposed for the election of $P \in \Omega$. We can mention techniques based on symbolic dynamics (Mischaikow, Mrozek, Reiss and Szymczak, 1999), Fourier analysis (Powell and Percival, 1979), and wavelet transform (Rosso and Mairal, 2002) among others. The applicability of these approaches depends on the data-characteristics, i.e., stationarity, length of the series, parameter-variations, levels of noise-contamination, etc. The distinct treatments at hand "capture" the global aspects of the dynamics, but they are not equivalent in their ability to discern physical details. However, one should recognize that we are here referring to techniques defined in an ad-hoc fashion, not derived directly from the dynamical properties of pertinent systems themselves.

López-Ruiz, Mancini and Calbet (LMC) (López-Ruiz et al., 1995), advanced a new statistical complexity measure (SCM), based on the notion of "disequilibrium", as a quantifier of the degree of physical structure in a time series. Given a probability distribution associated with a system's state, the LMC measure is the product of a normalized entropy H times a distance

to the uniform-equilibrium state Q. It vanishes both for a totally random process and for a periodic one. Martín et al. (Martín, Plastino and Rosso, 2003) improved on this measure by modifying the distance-component (in the concomitant probability space). In Ref. (Martín et al., 2003), Q is built-up using Wootters' statistical distance while H is a normalized Shannon-entropy. The ensuing statistical complexity measure is neither an intensive nor an extensive quantity, although it does yield an impressive quantity of useful results. A complexity measure should be able to distinguish among different degrees of periodicity and it should vanish only for periodicity unity. In order to attain such goals it would seem desirable to give this statistical measure an intensive character. This was achieved in Ref. (Lamberti et al., 2004), obtaining a SCM that is *(i)* able to grasp essential details of the dynamics, *(ii)* an intensive quantity, and *(iii)* capable of discerning among different degrees of periodicity and chaos.

By using the LMC definition (López-Ruiz et al., 1995) and the SCM defined in Ref. (Lamberti et al., 2004), we investigate here the classical limit of quantum mechanics (CLQM) of a semi-classical model containing both classical and quantum degrees of freedom in Ref. (Kowalski et al., 2002). In contrast to what was done in the above mentioned papers via a master equation for the density operator (Brun, 2000; Zurek et al., 1993; Habib et al., 1998), or by recourse to equivalent stochastic equations for pertinent expectation values (Ghose et al., 2003; Ghose et al., 2004), we consider a simplified scheme in which the interaction with the environment is simulated by the classical variables.

In the next section we consider a semiclassical system that represents a matter-field interaction. We analyze the corresponding dynamics and describe the quantum-classical transition zones.

Section 3 is dedicated to the Statistical Complexity concept. The LMC and SCM definitions are considered. Section 4 is devoted to discuss the results by considering two different approaches for the probability distribution, namely, relative wavelet energy and permutation patterns. Finally, in Section 5 we draw conclusions.

2 The CLQM for a special semi-classical model

We deal with a special bipartite system that represents the zero-th mode contribution of a strong external field to the production of charged meson pairs (Cooper et al., 1998; Kowalski et al., 2002), whose Hamiltonian reads

$$\hat{H} \;=\; \frac{1}{2}\left(\;\frac{\hat{p}^2}{m_q} \;+\; \frac{{P_A}^2}{m_{cl}} \;+\; m_q\omega^2\hat{x}^2\;\right), \tag{2.1}$$

where *i)* $\hat{x}$ and $\hat{p}$ are quantum operators, *ii)* A and P_A classical canonical conjugate variables and *iii)* $\omega^2 = {\omega_q}^2 + e^2A^2$ is an interaction term that introduces nonlinearity, ω_q being a frequency. The quantities m_q and m_{cl} are masses, corresponding to the quantum and classical systems, respectively. As shown in Ref. (Kowalski, Martín, Nuñez, Plastino and Proto, 1998), in dealing with Eq. (2.1) one faces an autonomous system of nonlinear coupled equations

$$\begin{array}{lll} \frac{d\langle\hat{x}^2\rangle}{dt} = \frac{\langle\hat{L}\rangle}{m_q}, & \frac{d\langle\hat{p}^2\rangle}{dt} = -m_q\,\omega^2\langle\hat{L}\rangle, & \frac{d\langle\hat{L}\rangle}{dt} = 2\left(\frac{\langle\hat{p}^2\rangle}{m_q} - m_q\,\omega^2\langle\hat{x}^2\rangle\right), \\ \frac{dA}{dt} = \frac{P_A}{m_{cl}}, & \frac{dP_A}{dt} = -e^2 m_q\,A\langle\hat{x}^2\rangle, & \end{array} \tag{2.2}$$

where $\hat{L} = \hat{x}\hat{p} + \hat{p}\hat{x}$. The system of Eq. (2.2) follows immediately from Ehrenfest's relations (Kowalski et al., 1998). To study the classical limit we also need to consider the classical counterpart of the Hamiltonian given by Eq. (2.1)

$$H = \frac{1}{2}\left(\frac{p^2}{m_q} + \frac{{P_A}^2}{m_{cl}} + m_q\omega^2 x^2\right), \tag{2.3}$$

where all the variables are classical. Recourse to Hamilton's equations allows one to find the classical version of Eq. (2.2) (see Ref. (Kowalski et al., 1998) for further details). These equations are identical in form to Eq. (2.2) after suitable replacement of quantum mean values by classical variables, i.e., $\langle\hat{x}^2\rangle \Rightarrow x^2$, $\langle\hat{p}^2\rangle \Rightarrow p^2$ and $\langle\hat{L}\rangle \Rightarrow L = 2xp$. The classical limit is obtained by letting the "relative energy"

$$E_r = \frac{E}{I^{1/2}\omega_q} \to \infty, \tag{2.4}$$

($E_r \geq 1$), where E is the total energy of the system and I is an invariant of the motion described by the system of equations previously introduced (Eq. (2.2)), related to the Uncertainty Principle

$$I = \langle\hat{x}^2\rangle\langle\hat{p}^2\rangle - \frac{\langle\hat{L}\rangle^2}{4} \geq \frac{\hbar^2}{4}. \tag{2.5}$$

A classical computation of I yields $I = x^2p^2 - L^2/4 \equiv 0$. Thus, I vanishes when it is evaluated using the classical variables A and P_A, for all t, i.e. $I(A, P_A) = 0$, a fact that exhibits the self-consistency of our methodology. A measure of the degree of convergence between classical and quantum results in the limit of Eq. (2.4) is given by the norm $\mathcal{N}$ of the vector $\Delta u = u - u_{cl}$ (Kowalski et al., 1998)

$$\mathcal{N}_{\Delta u} = |u - u_{cl}|, \tag{2.6}$$

where the three components vector $u = (\langle\hat{x}^2\rangle, \langle\hat{p}^2\rangle, \langle\hat{L}\rangle)$ is the "quantum" part of the solution of the system defined by Eq. (2.2) and $u_{cl} = (x^2, p^2, L)$ its classical counterpart.

A detailed study of this model, was performed in Refs. (Kowalski et al., 1998; Kowalski et al., 2002). The main results of these references, pertinent for our discussion, can be succinctly detailed as follows: in plotting diverse dynamical quantities as a function of E_r (as it grows from unity to ∞), one finds *an abrupt change in the system's dynamics for a special value of E_r, to be denoted by ${E_r}^{cl} = 21.55264$.* From this value onwards, the pertinent dynamics starts converging to the classical one. It is thus possible to assert that ${E_r}^{cl}$ provides us with an *indicator* of the presence of a quantum-classical "border". The zone

$$E_r < {E_r}^{cl}, \tag{2.7}$$

corresponds to the semi-quantal regime investigated in Ref. (Kowalski et al., 2002). This regime, in turn, is characterized by *two* different sub-zones (Kowalski et al., 2002). One of them is an almost purely quantal one, in which the microscopic quantal oscillator is just slightly perturbed by the classical one, and the other section exhibits a transitional nature (semi-quantal). The border between these two sub-zones can be well characterized by a relative energy value ${E_r}^{\mathcal{P}} = 3.3282$. A significant feature of this point resides in the fact that, for $E_r \geq {E_r}^{\mathcal{P}}$, *chaos is always found*. The relative number of chaotic orbits (with respect to the total number of orbits) grows with E_r and tends to unity for $E_r \to \infty$ (Kowalski et al., 2002).

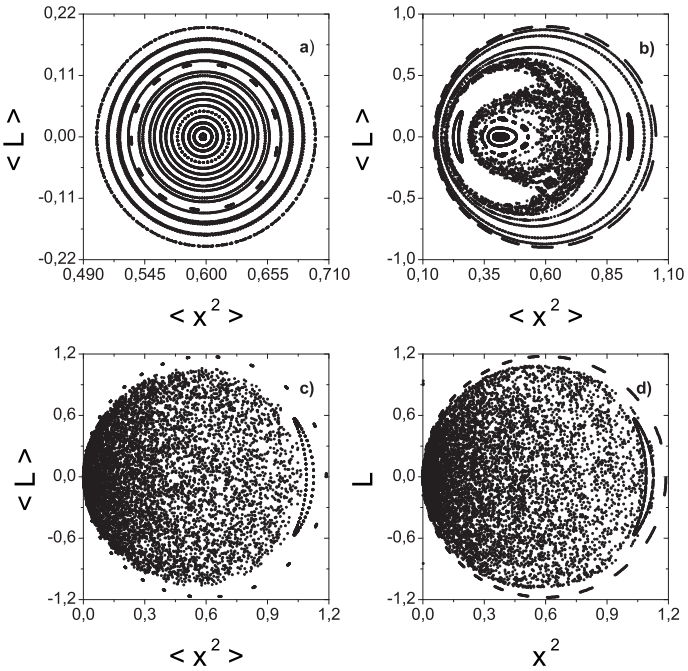

Figure 1: Poincaré surfaces of section: $\langle \hat{L} \rangle$ vs. $\langle \hat{x}^2 \rangle$, for $E = 0.6$, $A(t=0) = 0$, $m_q = m_{cl} = \omega_q = e = 1$. E_r adopts the following values: *a)* $1,0142$ ("quantum-like" regime), *b)* $3,5492$ (semi-classical regime), *c)* $24,2452$ (convergence to the classical limit is noticeable), *d)* $I = 0$ (classical instance).

In Figs. 1 we plot Poincaré surfaces of section corresponding to $\langle \hat{L} \rangle$ vs. $\langle \hat{x}^2 \rangle$, for $E = 0.6$, $A(t=0) = 0$, $m_q = m_{cl} = \omega_q = e = 1$. In Fig 1.a ($E_r = 1,0142$) we can observe quasiperiodic curves corresponding to the "quantum-like" regime. Fig. 1.b ($E_r = 3,5492$) corresponds to the semi-classical regime in the transition zone. We can see chaotic areas and non chaotic areas but with complex dynamics. Fig. 1.c ($E_r = 24,2452$) represents a case in the classical zone where the convergence to the classical results (shown in Fig. 1.d) becomes noticeable. Figs. 1.c and 1.d show both a chaotic phase space unless isolated islands of stability.

Thus, as E_r grows from $E_r = 1$ (the "pure quantum instance") to $E_r \to \infty$ (the classical situation), a significant series of *morphology changes* is detected, specially in the transition-zone (${E_r}^{\mathcal{P}} \leq E_r \leq {E_r}^{cl}$). The concomitant orbits exhibit features that are not easily describable in terms of Eq. (2.6), which is a *global* measure of the degree of convergence in amplitude (of the signal). What one needs instead is *a statistical type of characterization*, involving the notions of entropy and statistical complexity (Kowalski, Martín, Plastino, Proto and Rosso, 2003; Kowalski, Martín, Plastino and Rosso, 2005; Kowalski, Martín, Plastino and Rosso, 2007).

3 Statistical complexity

The Statistical Complexity can be viewed as a functional $C[P]$ that characterizes the probability distribution P associated to the time series generated by the dynamical system under study. It quantifies not only randomness but also the presence of correlational structures (López-Ruiz et al., 1995; Lamberti et al., 2004; Martín et al., 2003). This quantity introduced by López-Ruiz, Mancini and Calbet is of the form (López-Ruiz et al., 1995)

$$C_{LMC}[P] = D[P] \cdot H[P] \ , \tag{3.1}$$

where H is the normalized Shannon's entropy and $D[P]$ is the so-called "disequilibrium" defined as

$$D[P] = D_0 \sum_{i=1}^{n} \left(p_i - \frac{1}{N} \right)^2 , \tag{3.2}$$

i.e. the quadratic distance of the probability distribution $P \equiv \{p_i\}$ to the equiprobability, i.e. to the uniform distribution $P_e \equiv \{p_i = 1/N\}$. D_0 is a normalization constant such that $0 \leq D \leq 1$, given by

$$D_0 = N/(N-1) \ . \tag{3.3}$$

In Ref. (Lamberti et al., 2004) an alternative definition of the LMC-ideas is implemented via a quantifier

$$C_{JS}[P] = Q[P, P_e] \cdot H_S[P] \ , \tag{3.4}$$

where, to the probability distribution P, we associate the normalized entropic measure $H_S[P] = S[P]/S_{max}$, with $S_{max} = S[P_e]$ ($0 \leq H_S \leq 1$). S stands for any entropic form. We take here the disequilibrium Q to be defined in terms of the extensive Jensen divergence (Lamberti et al., 2004) according to

$$Q \equiv Q_J[P, P_e] = Q_0 \{ S[(P + P_e)/2] - S[P]/2 - S[P_e]/2 \}. \tag{3.5}$$

with

$$Q_0 \ = \ -2 \left\{ \left(\frac{N+1}{N} \right) \ln(N+1) - 2\ln(2N) + \ln N \right\}^{-1} , \tag{3.6}$$

a normalization constant that makes $0 \leq Q_J \leq 1$.

This SCM-version is *(i)* able to grasp essential details of the dynamics, *(ii)* an intensive quantity, and *(iii)* capable of discerning among different degrees of periodicity and chaos.

In the next Section we will show the results of applying both (3.1) and (3.4) to the quantum-classical transition of Section 2, 1) by recourse to a wavelet analysis and 2) by employing the Bandt and Pompe, permutational entropy approach (Bandt and Pompe, 2002; Bandt and Shiha, 2007).

4 Results

In obtaining our numerical results we chose $m_q = m_{cl} = \omega_q = e = 1$ for the system's parameters. For the initial conditions needed to tackle our system (Eq. (2.2)) we took $E = 0.6$, i.e., we fixed E and then varied I so as to obtain our different E_r-values. We took 41 values of

I. Additionally, we set $\langle L\rangle(0) = L(0) = 0$, $A(0) = 0$ (both in the quantum and the classical instances). $\langle x^2\rangle(0)$ takes values in the interval $x^2(0) < \langle x^2\rangle(0) \leq 0.502$, with $x^2(0) = 0.012$.
A main task is that of ascertaining which is the probability distribution P to be employed in (3.1) and (3.4). A possible option is that of performing a frequency-analysis or wave-decomposition. Wavelet analysis (WA) is in general considered more convenient than recourse to a Fourier-one, since the former provides adaptive time-frequency localization. Thus, WA is the better approach of the two for describing non-periodic or non-quasiperiodic dynamics, which is our case for almost all the E_r-range (see Section 2), a situation that really makes Fourier a non useful technique. A different option is that of symbolic coding, that will be discussed below. A third possibility is a traditional histogram approach, but we do not consider it here. Exhaustive comparison between the histogram's approach and the Bandt and Pompe one has been reported by Rosso et al. (Rosso, De Micco, Plastino and Larrondo, 2010).

4.1 Wavelet Analysis

Wavelet analysis (Mallat, 1999; Samar, Bopardikar, Rao and Swartz, 1999) is a method which relies on the introduction of an appropriate basis and a characterization of the signal by the amplitude-distribution in this basis. If the basis is required to be a proper orthogonal basis, any arbitrary function can be uniquely decomposed and the decomposition can be inverted (Mallat, 1999; Samar et al., 1999). Wavelet analysis is a suitable tool for detecting and characterizing specific phenomena in the time vs. frequency plane.
This method expresses our original time series in terms of a set $\Psi_{j,k}(t) = 2^{j/2}\Psi(2^j t - k)$, with $j,\ k\ \in \mathcal{Z}$ (the set of integers), of translations and scaling functions of a wavelet mother Ψ. In the case that this family is an orthonormal basis for the space of finite-energy functions, the concept of energy becomes linked with the usual notions derived from Fourier's theory. In our numerical analysis we use orthogonal cubic spline functions as the mother wavelet. Among several alternatives the symmetric and orthogonal wavelet basis obtained from it has become a recommendable tool for representing natural signals (Thevenaz, Blue and Unser, 2000).
The wavelet analysis is carried out over N_J, frequency resolution levels (denoted by index j, Daubechies' notation $j = -N_J, \cdots, -1$). The wavelet transform allows us a useful characterization of the signal (time series) by the amplitude distribution of the coefficients in the wavelet basis (Mallat, 1999; Samar et al., 1999). The j-scale wavelet coefficients family set $\{C_j(k)\}$ could be interpreted as the local residual errors between successive signal approximations at levels j and $j+1$. It contains information on the signal $\mathcal{S}(t)$ corresponding to the frequencies $(2j-1)\omega_s \leq |\omega| \leq (2j)\omega_s$, where ω_s represent the sample frequency.
The energy associated with j-resolution wavelet level, is given by

$$\varepsilon_j \ = \ \sum_k \ |C_j(k)|^2 \ . \tag{4.1}$$

Summing over all the available wavelet levels j we obtain the total energy

$$\varepsilon_{tot} \ = \ \sum_{j=-N_J}^{-1} \ \varepsilon_j \ . \tag{4.2}$$

Finally, we define the relative wavelet energy as

$$\rho_j = \varepsilon_j / \varepsilon_{tot} \ . \tag{4.3}$$

The relative wavelet energy associated to the different frequency bands enables one to learn about their relative degree of importance. This time-scale probability distribution of energy across the frequency scales, $P = \{\rho_j\}$, constitutes a suitable tool for detecting and characterizing specific phenomena in both time and frequency planes. Then, if one is in possession of a probability distribution, the possibility of applying Information Theory allows us to evaluate specific quantifiers like the Normalized Total Shannon Entropy and the Statistical Complexity measures which could give additional information about the dynamical process under study.

The first task is to evaluate the wavelet energy probability distribution $P = \{\rho_i\}$ to be employed in (3.1) and (3.4). Our data points are the solutions of (2.2), from which we extract the values of $\langle x^2 \rangle$ and the (classical) values of x^2 at the time t (for a fixed E_r) (We have also performed these calculations extracting instead the quantities $\langle p^2 \rangle$ - p^2 together with $\langle L \rangle$ - L, and obtained thereby entirely similar results to those reported below). We will deal with 2^{12} data-points, for each orbit. We define eight ($N_J = 8$) resolution levels $j = -1, -2, \cdots, -N_J$ for a multi-resolution wavelet analysis.

We find, as first result, that both C_{LMC} and C_{JS} correctly *distinguish* the three well-known physical zones or sections of our process, i.e., quantal, transitional, and classic, as delimited by, respectively, ${E_r}^{\mathcal{P}}$ and ${E_r}^{cl}$. Notice please the abrupt change in the slope of the curve of Figs. 2 taking place at ${E_r}^{\mathcal{P}}$, where a local minimum is detected for C_{LMC} and C_{JS} (Figs. 2). The transition zone is clearly demarcated between that point and ${E_r}^{cl}$. From there on C_{LMC} and C_{JS} tend to their classical values at the same time that the quantum solutions of (2.2) begin to converge towards the classical counterparts.

In the quantum-classic route, an important milestone is found at $E_r = E_r^M$. This point can be detected, within the transition zone, at the value $E_r^M = 6,8155$, where an absolute maximum can be appreciated (Figs. 2) for both C_{LMC} and C_{JS}.

There are however some transition-details that are not well represented by neither C_{LMC} nor C_{JS}, that fail in trying to describe the quantal region. Here both the quantum zone and the classical one should exhibit similar degrees of complexity, smaller than those for the transition zone, as the pertinent dynamics are, respectively, quasiperiodic in the quantum instance (Fig. 1.a) and chaotic in the classic one (Fig. 1.c). In the phase space corresponding to the transition zone coexist sectors of chaotic dynamics with others of more complex nature, neither chaotic nor quasiperiodical (Fig. 1.b). In the classical zone C_{LMC} and C_{JS} are smaller than in the transition zone, as one would expect. This is not always so in the quantum zone, that is, for all E_r. The C_{LMC} description is better than the C_{JS} one, as the latter diminishes for $E_r \to 1$, as it should.

The quantal is the zone where one expects poor results from wavelet analysis, because there a superposition of frequencies takes place. These difficulties will be overcome in the next Section using the so-called Bandt and Pompe approach for evaluating the probability distribution P associated to the time series under study, a symbolic technique.

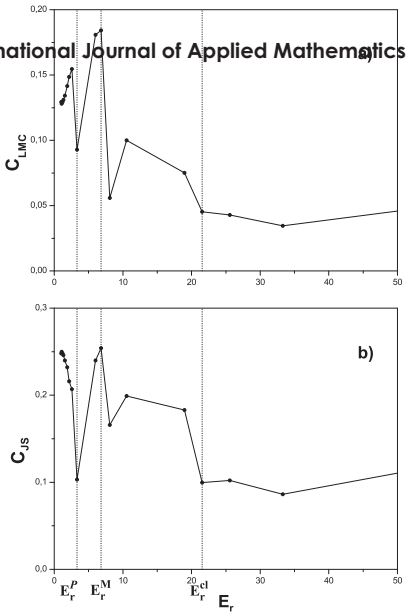

Figure 2: *a)* $\mathcal{C}_{LMC}$ and *b)* $\mathcal{C}_{JS}$ vs. E_r. Both quantities evaluated by performing a wavelet-band analysis. Three zones are to be differentiated, quantal, transition, and classical. They are delimited by special E_r values, namely, ${E_r}^{\mathcal{P}} = 3.3282$ and ${E_r}^{cl} = 21,55264$. Notice the complexity maximum at the same E_r value, $E_r^M \simeq 6,8155$.

4.2 Bandt Pompe Approach

The symbolic methodology proposed by Bandt and Pompe (Bandt and Pompe, 2002) is based on the details of the series time delay reconstruction procedure. Here, causal, dynamic information should be expected to help getting better results. The essence of symbolic dynamics is to associate a symbol sequence with each trajectory of a continuous or discrete dynamical system, by means of a suitable partition of the state-space. The new symbolic series are obtained by reordering the amplitude values of the original time series x_i. Consider the sequence of amplitude values associated to the time series x_i with embedding dimension $D > 1$ and time delay τ given by

$$x_i \mapsto \left(x_{i-(D-1)\tau}, x_{i-(D-2)\tau}, \ldots, x_{i-\tau}, x_i\right). \tag{4.4}$$

To each time i we are assigning a D-dimensional vector that results from the evaluation of the time series at times $i, i-\tau, \ldots, i-(D-1)\tau$. Clearly, the greater the D value, the more information about the past is incorporated into the ensuing vectors. By the ordinal pattern of order D related to the time i we mean the permutation $\hat{x}_i = (r_0, r_1, \cdots, r_{D-1})$ of $(0, 1, \cdots, D-1)$ defined by

$$x_{i-r_{D-1}\tau} \leq x_{i-r_{D-2}\tau} \leq \cdots \leq x_{i-r_1\tau} \leq x_{i-r_0\tau}. \tag{4.5}$$

In this way the vector defined by Eq. (4.4) is converted into a unique symbol $\hat{x}_i$. Further details about the Bandt and Pompe method can be found in Ref. (Bandt and Shiha, 2007). For all the $D!$ possible permutations $\hat{x}_i$ of order D, their associated relative frequencies can be naturally

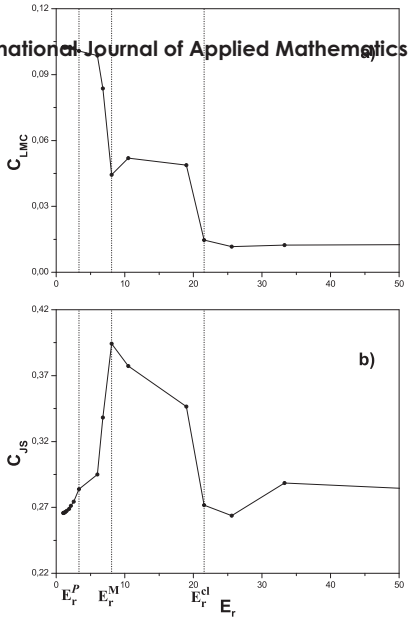

Figure 3: Statistical Complexities, *a)* $\mathcal{C}_{LMC}$ and *b)* $\mathcal{C}_{JS}$ vs. E_r. We consider here the Symbolic version. As in Fig. 2, we can observe the three zones of the process, quantal, transition, and classical, delimited by ${E_r}^{\mathcal{P}} = 3.3282$ and ${E_r}^{cl} = 21,55264$, but only $\mathcal{C}_{JS}$ attains a maximum in the transition zone, now at $E_r^M = 8,0904$. The Jensen-Shannon Complexity $\mathcal{C}_{JS}$ is smaller in the quantal zone where the dynamics is quasiperiodic, and in the classical zone (where it is chaotic), than in the transition zone of complex dynamics, as expected.

computed by

$$p(\hat{x}_i) = \frac{\sharp\{i|1+(D-1)\tau \leq i \leq N \text{ and } i \text{ has ordinal pattern } \hat{x}_i\}}{N-(D-1)\tau}, \tag{4.6}$$

where $\sharp$ is the cardinality of the set—roughly speaking, the number of elements in it. Thus, a permutation probability distribution $P_x = \{p(\hat{x}_i), i = 1, \ldots, D!\}$ is obtained from the time series x_i. The probability distribution P is obtained once we fix the embedding dimension D and the time delay τ. The former parameter plays an important role for the evaluation of the appropriate probability distribution, since D determines the number of accessible states, $D!$, and tells us about the necessary length N of the time series needed in order to work with a reliable statistics. In particular, Bandt and Pompe (Bandt and Pompe, 2002) suggest for practical purposes to work with $3 \leq D \leq 7$.

Here the value $D = 5$ was selected. As we will deal with vectors with components of at least $N = 5000$ data-points for each orbit, the condition $N \gg D!$ is clearly satisfied. We take the customary time delay $\tau = 1$ (Bandt and Pompe, 2002). We find again, that both C_{LMC} and C_{JS} distinguishes the three sections of our process, i.e., quantal, transitional, and classic. Also for $E_r > {E_r}^{cl}$, C_{LMC} and C_{JS} tend to their classical values at the same time that the solutions of Eq. (2.2) begin to converge towards the classical ones.

However, C_{LMC} is no longer maximal within the transition zone and its performance becomes

worse for the quantal one, where it attains maximal values (Fig. 3.a). Instead, C_{JS} is maximal where it should, i.e., within the transition zone. Moreover, C_{JS} exhibits similar small values in the quantum zone and in the classical one. More importantly, these values are clearly smaller than those pertaining to the transition zone, overcoming thus the above mentioned wavelet-associate anomaly (Fig. 3.b). Of course, the complexity cannot vanish neither in the quantum zone, because we deal there with a frequency superposition (non-periodic dynamics), nor in the classical one, due to the chaotic character of the associated motion (obviously, chaotic and random are not equivalent concepts in this respect). The absolute maximum of C_{JS} is found within the transition region, at the value $E_r^M = 8,0904$ (Fig. 3.b), an E_r-value at which great alterations in the system's dynamics ensue, indeed, in the solutions of (2.2) (Kowalski et al., 2002). E_r^M divides approximately into two sections the transitional region, one in which the quantum-classical mixture characterizes a phase-space with more non-chaotic than chaotic curves and other, in which this feature is reversed (Kowalski et al., 2002). We thus find that the symbolic $C_{JS}-$ version optimizes the description of the quantum-classical transition corresponding to the semiclassical model of Section 2.

5 Conclusions

In the present work we have studied the classical-quantal frontier problem by using two definitions of the LMC notion of Statistical Complexity (López-Ruiz et al., 1995). We dealt with the dynamics generated by a semi-classical Hamiltonian that represents the zero-th mode contribution of a strong external field to the production of charged meson pairs (Cooper et al., 1998; Kowalski et al., 2002).

Another central aspect is that of determining the correct probability distribution to be associated to the pertinent time series, which was attempted via two quite different approaches, namely, the analog wavelet analysis and the symbolic Bandt and Pompe approach.

We find, as first result, that by recourse to a wavelet analysis, both C_{LMC} and C_{JS} given by Eqs. (3.1) and (3.4) correctly *distinguish* the three zones or sections of our process, i.e., quantal, transitional, and classic, as delimited by, respectively, ${E_r}^{\mathcal{P}}$ and ${E_r}^{cl}$ (Figs. 2). In both cases the maximum maximorum lies within the transition zone. However, both representations fail to adequately describe the quantal region, although the failure is less notorious in the $C_{LMC}-$ instance (Fig. 2.a). These inadequacies are overcome only in the C_{JS} case, by recourse to the symbolic Bandt and Pompe approach. C_{JS} correctly *distinguishes and represents* the three zones of the quantum classical-transition (Fig. 3.b), characterized by a quasiperiodic dynamics (quantal zone), a chaotic one (classical zone) and a transition region where one detects coexistence of sectors of chaotic dynamics with others of a more complex nature, neither chaotic nor quasiperiodical (Fig. 1.b). The Statistical Complexity maximum maximorum lies at the transition zone, for $E_r^M = 8,0904$. This particular E_r^M divides approximately into two sections the transitional region, one in which the quantum-classical mixture characterizes a phase-space with more non-chaotic than chaotic curves and other, in which this feature is reversed (Kowalski et al., 2002).

Summing up, the symbolic C_{JS} optimizes the phenomenal description of the physics governed

by the Hamiltonian Eq. (2.1). The essential point is revealed here to be just how one extracts, from the pertinent time-series, the underlying probability distribution to be employed in evaluating information-theoretic quantifiers.

Acknowledgment

A. M. Kowalski is supported by CIC of Argentina. O. A. Rosso acknowledges partial support from CONICET, Argentina, and CAPES, PVE fellowship, Brazil.

References

Bandt, C. and Pompe, B. 2002. Permutation entropy: A natural complexity measure for time series, *Phys. Rev. Lett.* **88**: 174102.

Bandt, C. and Shiha, F. 2007. Order patterns in time series, *Journal of Time Series Analysis* **28**: 646–665.

Bloch, F. 1946. Nuclear induction, *Phys. Rev.* **70**: 460–474.

Bonilla, L. L. and Guinea, F. 1992. Collapse of the wave packet and chaos in a model with classical and quantum degrees of freedom, *Phys. Rev. A* **45**: 7718–7728.

Brun, T. A. 2000. Continuous measurements, quantum trajectories, and decoherent histories, *Phys. Rev. A* **61**: 042107.

Brun, T. A. and Halliwell, J. J. 1996. Decoherence of hydrodynamic histories: A simple spin model, *Phys. Rev. D* **54**: 2899–2912.

Clark, T. D., Diggins, J., Ralph, J. F., Everitt, M., Prance, R. J., H., P., Whiteman, R., Widom, A. and Srivastava, Y. N. 1998. Coherent evolution and quantum transitions in a two level model of a SQUID ring, *Annals of Physics* **268**: 1–30.

Cooper, F., Dawson, J., Habib, S. and Ryne, R. D. 1998. Chaos in time-dependent variational approximations to quantum dynamics, *Phys. Rev. E* **57**: 1489–1498.

Diósi, L., Gisin, N., Halliwell, J. and Percival, I. C. 1995. Decoherent histories and quantum state diffusion, *Phys. Rev. Lett.* **74**: 203–207.

Everitt, M. J. 2007. Recovery of classical chaotic-like behavior in a conservative quantum three-body problem, *Phys. Rev. E* **75**: 036217.

Everitt, M. J., Munro, W. J. and Spiller, T. P. 2009. Quantum-classical crossover of a field mode, *Phys. Rev. A* **79**: 032328.

Ghose, S., Alsing, P., Deutsch, I., Bhattacharya, T. and Habib, S. 2004. Transition to classical chaos in a coupled quantum system through continuous measurement, *Phys. Rev. A* **69**: 052116.

Ghose, S., Alsing, P., Deutsch, I., Bhattacharya, T., Habib, S. and Jacobs, K. 2003. Recovering classical dynamics from coupled quantum systems through continuous measurement, *Phys. Rev. A* **67**: 052102.

Greenbaum, B. D., Habib, S., Shizume, K. and Sundaram, B. 2005. The semiclassical regime of the chaotic quantum-classical transition, *Chaos* **15**: 033302.

Habib, S., Shizume, K. and Zurek, W. H. 1998. Decoherence, chaos, and the correspondence principle, *Phys. Rev. Lett.* **80**: 4361–4365.

Halliwell, J. J. and Yearsley, J. M. 2009. Arrival times, complex potentials, and decoherent histories, *Phys. Rev. A* **79**: 062101.

Katz, I., Retzker, A., Straub, R. and Lifshitz, R. 2007. Signatures for a classical to quantum transition of a driven nonlinear nanomechanical resonator, *Phys. Rev. Lett.* **99**: 040404.

Kociuba, G. and Heckenberg, N. R. 2002. Controlling the complex Lorenz equations by modulation, *Phys. Rev. E* **66**: 026205.

Kolmogorov, A. N. 1958. A new metric invariant of transitive dynamic system and automorphysms in lebesgue spaces, *Dokl. Akad. Nauk. SSSR* **119**: 861.

Kowalski, A. M., Martín, M. T., Nuñez, J., Plastino, A. and Proto, A. N. 1998. Quantitative indicator for semiquantum chaos, *Phys. Rev. A* **58**: 2596–2599.

Kowalski, A. M., Martín, M. T., Plastino, A., Proto, A. N. and Rosso, O. A. 2003. Wavelet statistical complexity analysis of classical limit, *Phys. Lett. A* **311**: 180–191.

Kowalski, A. M., Martín, M. T., Plastino, A. and Rosso, O. A. 2005. Entropic non-triviality, the classical limit, and geometry-dynamics correlations, *Int. J. of Modern Phys. B* **14**: 2273–2285.

Kowalski, A. M., Martín, M. T., Plastino, A. and Rosso, O. A. 2007. Bandt-pompe approach to the classical-quantum transition, *Physica D* **233**: 21–31.

Kowalski, A. M., Plastino, A. and Proto, A. N. 2002. Classical limits, *Phys. Lett. A* **297**: 162–172.

Lamberti, P. W., Martín, M. T., Plastino, A. and Rosso, O. A. 2004. Intensive entropic nontriviality measure, *Physica A* **334**: 119–131.

López-Ruiz, R., Mancini, H. L. and Calbet, X. 1995. A statistical measure of complexity, *Phys. Lett. A* **209**: 321–326.

Mallat, S. 1999. *A wavelet tour of signal processing*, University Press, Cambridge.

Martín, M. T., Plastino, A. and Rosso, O. A. 2003. Statistical complexity and disequilibrium, *Phys. Lett. A* **311**: 126–132.

Meystre, P. and Sargent III, M. 1991. *Elements of Quantum Optics*, Springer-Verlag.

Milonni, P., Shih, M. and Ackerhalt, J. R. 1987. *Chaos in Laser-Matter Interactions*, World Scientific Publishing Co.

Mischaikow, K., Mrozek, M., Reiss, J. and Szymczak, A. 1999. Construction of symbolic dynamics from experimental time series, *Phys. Rev. Lett.* **82**: 1114–1147.

Powell, G. E. and Percival, I. C. 1979. A spectral entropy method for distinguishing regular and irregular motion of hamiltonian systems, *J. Phys. A: Math. Gen.* **12**: 2053–2071.

Ring, P. and Schuck, P. 1980. *The Nuclear Many-Body Problem*, Springer-Verlag.

Rosso, O. A., De Micco, L., Plastino, A. and Larrondo, H. A. 2010. Info-quantifiers' map-characterization revisited, *Physica A* **389**: 4604–4612.

Rosso, O. A. and Mairal, L. 2002. Characterization of time dynamical evolution of electroencephalographic records, *Physica A* **312**: 469–504.

Samar, V., Bopardikar, A., Rao, R. and Swartz, K. 1999. Wavelet analysis of neuroelectric waveforms: a conceptual tutorial, *Brain Lang* **66**: 7–60.

Shannon, C. E. 1948. A mathematical theory of communication, *Bell Syst. Technol. J.* **27**: 379–423; 623–56.

Shiner, J. S., Davison, M. and Landsberg, P. T. 1999. Simple measure for complexity, *Phys. Rev. E* **59**: 1459–1464.

Sinai, Y. G. 1959. On the concept of entropy of dynamical system, *Dokl. Akad. Nauk. SSSR* **124**: 768–771.

Thevenaz, P., Blue, T. and Unser, M. 2000. Interpolation revisited, *IEEE Trans Med Imaging* **19**: 739758.

Zeh, H. D. 1999. Why bohm's quantum theory?, *Found. Phys. Lett.* **12**: 197–200.

Zurek, W. H. 1981. Pointer basis of quantum apparatus: Into what mixture does the wave packet collapse?, *Phys. Rev. D* **24**: 1516–1525.

Zurek, W. H. 2003. Decoherence, einselection, and the quantum origins of the classical, *Rev. Mod. Phys.* **75**: 715–775.

Zurek, W., Habib, S. and Paz, J. 1993. Coherent states via decoherence, *Phys. Rev. Lett.* **70**: 1187–1190.